Journal of Advanced Ceramics
2014, 3(3): 194–206
DOI: 10.1007/s40145-014-0110-4

ISSN 2226-4108
CN 10-1154/TQ

Research Article

Preparation, crystallization, microstructure and dielectric properties of lead bismuth titanate borosilicate glass ceramics

Chandkiram R. GAUTAM[a,*], Abhishek MADHESHIYA[a], Ranabrata MAZUMDER[b]

[a]*Advanced Glass and Glass Ceramic Research Laboratory, Department of Physics, University of Lucknow, Lucknow 226007, India*
[b]*Department of Ceramic Engineering, National Institute of Technology, Rouerkela 769008, India*

Received: April 10, 2014; Revised: May 15, 2014; Accepted: May 28, 2014

Abstract: Various bulk and transparent glasses were prepared by rapid melt quenching technique in the glass system $55[(Pb_xBi_{1-x})TiO_3]$–$44[2SiO_2B_2O_3]$–La_2O_3 (x=0–0.7). The X-ray diffraction (XRD) studies of the glass samples confirmed the amorphous nature. The differential thermal analyses (DTA) were carried out from room temperature to 900 ℃ with a heating rate of 10 ℃/min. The DTA patterns of the samples showed one or more exothermic sharp peaks shifting towards lower temperature side with increasing concentration of bismuth oxide (BiO). On the basis of DTA results, the solid solution of bismuth titanum oxide ($Bi_2Ti_2O_7$)/lead bismuth titanium oxide ($Pb_3Bi_4Ti_6O_{21}$) was precipitated in borosilicate glassy matrix as a major phase. The glasses were subjected to 4 h and 8 h heat treatment schedules to convert into glass ceramics. XRD analysis of these glass ceramic samples showed that the major crystalline phase of the entire glass ceramic samples with $0 \leqslant x \leqslant 0.5$ is found to have cubic crystal structure, while it is tetragonal for glass ceramic sample with x=0.7. The scanning electron microscopy (SEM) micrographs indicated the uniform distribution of $Bi_2Ti_2O_7$ and $Pb_3Bi_4Ti_6O_{21}$ crystallites in the glassy matrix.

Keywords: lead bismuth titanate; differential thermal analysis (DTA); crystallization; scanning electron microscopy (SEM); dielectric behavior

1 Introduction

From the last four decades, after the remarkable discovery by Aurivillius of a new family of materials named after his name, a concerted effort by the researchers resulted in the discovery of various novel glass ceramics containing ferroelectric crystals such as Bi_2WO_6, $BiTiO_3$, $(Na,K)NbO_3$, $BaTiO_3$, $Pb_5Ge_3O_{11}$, $LiNbO_3$, $Bi_2VO_{5.5}$, Bi_2GeO_5, solid solutions of $Pb_xBa_{1-x}TiO_3$ and $SrAl_2Si_2O_8$ embedded in glassy matrix [1–11]. The most important applications of Aurivillius family of bismuth based ferroelectric materials involve a layered structure in capacitors, sensors, and piezoelectric and electro-optic devices, which is strongly influenced by the method of preparation [12–15]. Out of different preparation methods, crystallization from the glasses has been applied to synthesize the glass ceramics [16–20]. This method gives possibility of doping with different cations to improve the properties of the glasses and glass ceramics. It also allows to control the particle size evolution during the transition from amorphous to crystalline state and to achieve suitable

* Corresponding author.
E-mail: gautam_ceramic@yahoo.com

crystallographic orientation in the polycrystalline materials [21]. SiO_2 is introduced to change the melting conditions, while Nd_2O_3 addition to bismuth titanate effectively improves the electrical properties [22–30]. The glass ceramic route of preparing $BiTiO_3$ is desirable to obtain the material and associated with pore free fine grains of microstructure embedded in the glassy matrix [2]. Besides controlling the crystallite size, this method also provides the control over the transparent characteristics of the parent glasses during the crystallization [31]. It was reported that glass nanocomposites comprising nanocrystallites of bismuth titanate (BiT), dispersed in a glassy matrix of strontium tetra borate (SrB_4O_7, SBO) achieved by the controlled crystallization of glasses [32]. It was observed that ultrasonic treatment (UST) of the glass samples with an aqueous suspension of BiT followed by conventional heat treatment yields the desired crystalline phase, which is otherwise difficult to obtain by conventional heat treatment. Gerth and Rüssel [18] have reported the crystallization behavior of BiT in the Bi_2O_3–TiO_2–B_2O_3 system. However, they have observed the tendency of spontaneous devitrification, and only samples with thickness of only 1 mm could be produced with the system by employing cooling rate as high as 227 ℃/min during casting of glass melt. Kojima *et al*. [16] prepared BiT glass ceramics by a twin-roller rapid quenching technique. Recently, the study on the fabrication of K_2O–SiO_2–Bi_2O_3–TiO_2 glasses in the silicate matrix has been reported. The glasses and their glass ceramics are produced by the simple conventional melt quenching technique followed by controlled heat treatment to obtain $BiTiO_3$ crystal containing glass ceramic nanocomposites in bulk quantity [33]. More recently, Golezardi *et al*. [34] reported their work on crystallization behavior, microstructure and dielectric properties of lead titanate glass ceramics in the presence of Bi_2O_3 as a nucleating agent.

The present paper focuses on the crystallization, microstructure and dielectric properties of glass ceramics with varying BiO content. According to our knowledge, there is no report for the preparation of glass ceramics containing the phases of solid solution of bismuth titanum oxide ($Bi_2Ti_2O_7$)/lead bismuth titanium oxide ($Pb_3Bi_4Ti_6O_{21}$) by melt quenching with participation of SiO_2 and La_2O_3, and the preparation, crystallization, microstructure and dielectric behavior of (Pb,Bi)TiO_3 borosilicate glass ceramic system have not been reported elsewhere either.

2 Materials and methods

2.1 Glass preparation

Analytical reagent grade chemicals PbO (Fisher Scientific, 99%), Bi_2O_3 (Himedia, 99.99%), TiO_2 (Himedia, 99%), SiO_2 (Himedia, 99.5%), H_3BO_3 (Himedia, 99.8%) and La_2O_3 (Himedia, 99.9%) were well mixed for 2 h in acetone media using mortar and pestle. Dried powders were melted in platinum crucible for 1 h in the temperature range of 1200–1270 ℃ under normal atmospheric condition depending on the composition. The melt was quenched by pouring it onto an aluminum mould and pressing with a thick aluminum plate. The glasses were then annealed at 400 ℃ for 4 h.

2.2 Density measurements

The density of the prepared glasses and glass ceramic samples has been calculated by Archimedes principle [35]. Distilled water was used as the liquid medium. The density of these glasses and glass ceramic samples is listed in Tables 1 and 2, respectively. The following formula was used for determination of the density of glass samples:

$$\text{Density} = \frac{W_2 - W_1}{(W_4 - W_1) - (W_3 - W_2)} \tag{1}$$

where W_1 is the weight of empty specific gravity bottle (g); W_2 is the weight of specific gravity bottle with sample (g); W_3 is the weight of specific gravity bottle with sample and distilled water (g); and W_4 is the weight of specific gravity bottle with distilled water (g). The density of distilled water is 1.0 g/cm^3.

2.3 X-ray diffraction measurements

X-ray diffraction (XRD) of powder glass samples was carried out using a Rigaku Miniflex-II X-ray diffractometer with Cu Kα radiation to check the amorphous state of the prepared glass samples.

2.4 Differential scanning calorimetry measurements

Differential scanning calorimetry (DSC) was done using a DSC equipment model NETZSCH STA 449C from room temperature (~27 ℃) to 900 ℃ employing a heating rate of 10 ℃/min to determine glass transition temperature T_g and crystallization

Table 1 Nomenclature of glass samples, their compositional distribution and glass transition temperature, DTA peak and density of various glass samples in the system $55[(Pb_xBi_{1-x})TiO_3]$–$44[2SiO_2B_2O_3]$–La_2O_3

Glass sample code	x	Composition (wt%)			Glass transition temperature T_g (℃)	Crystallization temperature T_c (℃)	Density (g/cm^3)
		$(Pb_xBi_{1-x})TiO_3$	$2SiO_2$–B_2O_3	La_2O_3			
BTL0.0	0.0	55	44	1	558	626	2.758
PBTL0.1	0.1	55	44	1	541	631	2.895
PBTL0.3	0.3	55	44	1	532	624	3.009
PBTL0.5	0.5	55	44	1	530	622	3.481
PBTL0.7	0.7	55	44	1	514	545, 629, 770	3.972

Table 2 Glass ceramic code, density, heating rate, holding time, holding temperature, crystal structure and crystalline phase

Glass ceramic code	Density (g/cm^3)	Heat treatment schedule			Crystal structure	Crystalline phase
		Heating rate (℃/min)	Holding time (h)	Holding temperature (℃)		
BTL0.0626F	2.765	5	4	626	Cubic	BTO
BTL0.0626E	2.785	5	8	626	Cubic	BTO
PBTL0.1631F	3.793	5	4	631	Cubic	BTO
PBTL0.1631E	3.796	5	8	631	Cubic	BTO
PBTL0.3624F	3.864	5	4	624	Cubic	BTO
PBTL0.3624E	3.875	5	8	624	Cubic	BTO
PBTL0.5622F	3.882	5	4	622	Cubic	BTO
PBTL0.5622E	3.888	5	8	622	Cubic	BTO
PBTL0.7629F	3.920	5	4	629	Tetragonal	PBTO
PBTL0.7629E	3.941	5	8	629	Tetragonal	PBTO
PBTL0.7770F	3.963	5	4	770	Tetragonal	PBTO
PBTL0.7770E	3.998	5	8	770	Tetragonal	PBTO

BTO—$Bi_2Ti_2O_7$ (bismuth titanum oxide); PBTO—$Pb_3Bi_4Ti_6O_{21}$ (lead bismuth titanium oxide).

temperature T_c. Sintered alumina was used as a reference material. On the basis of differential thermal analysis (DTA) results, various glass ceramic samples with compositions $x = 0$–0.5 were prepared by heat treating the glasses in the temperature range of 622–631 ℃ for 4 h and 8 h. The different heat treatment schedules and nomenclature of glass ceramic samples are listed in Table 2.

2.5 Nomenclature of glasses and glass ceramic samples

Five-letter glass codes refer to the composition of the glasses. First three letters PBT designate the content of lead bismuth titanate. The fourth letter L indicates that 1 wt% La_2O_3 is used as an additive, while the fifth letter, i.e., 0.0, 0.1, 0.3, 0.5 or 0.7, indicates the fraction of x in the glass system. For the nomenclature of the glass ceramic samples, the following methodology has been adopted. First five letters in the codes for the glass ceramic samples are similar to the codes of their parent glasses and refer to the composition of glasses, and the next three digits indicate the crystallization temperature. The last letter F or E refers to the holding time at crystallization temperature, 4 h and 8 h respectively. Take the glass ceramic sample PBTL0.1631F as an example: the first three letters represent the content of lead bismuth titanate, 0.1 represents the value of composition ($x = 0.1$), 631 is the crystallization temperature and F indicates the 4 h soaking time. Phases were identified using powder XRD analysis. Diffraction patterns were recorded employing a Rigaku X-ray diffractometer using Cu Kα radiation. The crystalline phases in each glass ceramic sample were identified by comparing its XRD pattern with standard patterns of various crystalline phases.

2.6 Polishing for scanning electron microscopy and dielectric measurements

The glass ceramic samples were ground and polished successively using SiC powders on a thick and flat glass plate. Finally polishing was carried out on a blazer cloth using diamond paste (1 μm). The polished glass ceramic samples were etched for 1 min with a suitable etchant (30%HNO_3 + 20%HF solution). Etched surface of various glass ceramic samples was coated with gold by sputtering method. The samples

were then examined using a JSM-840 scanning electron microscope (SEM) to study the morphology of different crystalline phases. Capacitance (C) and dissipation factor (D) were recorded as a function of temperature between room temperature and 500 ℃ at 0.1 kHz, 1 kHz, 10 kHz and 1 MHz using a Wayne Kerr 6500 P (high frequency LCR meter, frequency 20 Hz–5 MHz). The values of capacitance C and dissipation factor D were measured as a function of frequency at various temperatures.

3 Results and discussion

3.1 Density measurement analysis

Density of all the glasses and glass ceramic samples is listed in Tables 1 and 2, respectively. A systematic trend is observed in the values of density for all the glass samples. From Table 1, it is observed that the density of the glass samples for all the compositions (x = 0–0.7) increases with increasing concentration of PbO, because the density of Pb (11.4 g/cm^3) is much greater than the density of Bi (9.8 g/cm^3). The density of glass samples is found to lie in the range of 2.758–3.972 g/cm^3.

The measured density of the glass ceramic samples is listed in Table 2. It is observed that the density of the glass ceramic samples is found higher in comparison to the density of their parent glass samples. This is because during the crystallization or phase transformation change in volume results, it leads to a change in the specific gravity. The specific gravity of a glass ceramic is often different from that of the parent glass because of small volume changes that may occur during the heat treatment process. These changes may involve either a slight contraction or a slight expansion, but it would not usually exceed a 3% volume change. Hence the crystalline phases formed may have higher/lower densities than the original glass [36].

3.2 X-ray diffraction analysis of glass samples

Transparent bulk and thin glasses of optical quality with the composition 55[(Pb_xBi_{1-x})TiO_3]–44[($2SiO_2B_2O_3$)]–La_2O_3 (x = 0–0.7) in molar ratio were synthesized via a conventional melt quenching technique. All XRD patterns of various glass samples BTL0.0, PBTL0.1, PBTL0.3, PBTL0.5 and PBTL0.7 are shown in Fig. 1. These XRD patterns exhibit broad diffuse scattering at different angles instead of crystalline peaks, confirming a long range structural disorder characteristic of amorphous glassy network.

3.3 Differential thermal analysis

DTA curves of prepared glasses with different lead to bismuth ratios (x = 0–0.7) are shown in Fig. 2. The DTA patterns of glasses with compositions x = 0–0.5 show only one exothermic peak. These exothermic peaks represent the temperature at which the rate of crystallization of different phases is maximum. All glasses show a shift in the base line at different temperatures, depending on the compositions, in the temperature range of 514–558 ℃. These shifts in the base line show a change in the specific heat of the glasses, which is attributed to the glass transition temperature, T_g [37–40]. Glass transition temperatures of different glass samples are given in Table 1. The glass transition temperature has been found to decrease with decreasing concentration of BiO. This may be due to increase in the viscosity of the melt. With decrease in BiO content in the glass samples, the glassy network forming oxide SiO_2 reduces, and hence the viscosity of the glass and glass transition temperature T_g are decreased. It is reported by the previous researchers that with decreasing content of network-forming oxides, the glass transition temperatures are reduced. Due to the decrease of network-forming oxides in the glasses with the advent of bismuth titanate in the glasses, the viscosity and crosslinking are decreased [11]. The DTA pattern of the glass sample PBTL0.7 with composition x = 0.7 shows three different peaks

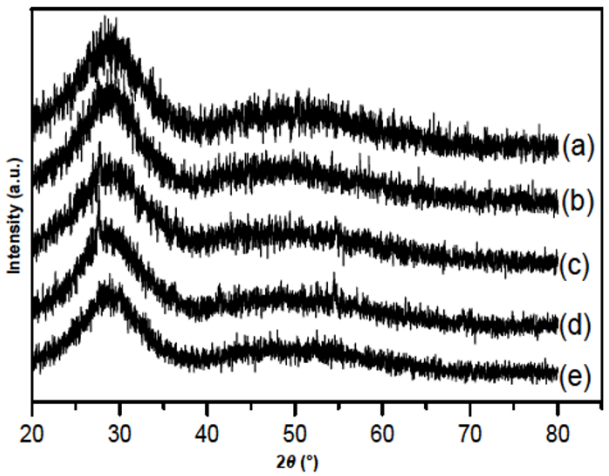

Fig. 1 XRD patterns of glass samples with (a) x = 0, (b) x = 0.1, (c) x = 0.3, (d) x = 0.5 and (e) x = 0.7 in the glass system 55[(Pb_xBi_{1-x})TiO_3]–44[$2SiO_2B_2O_3$]–La_2O_3.

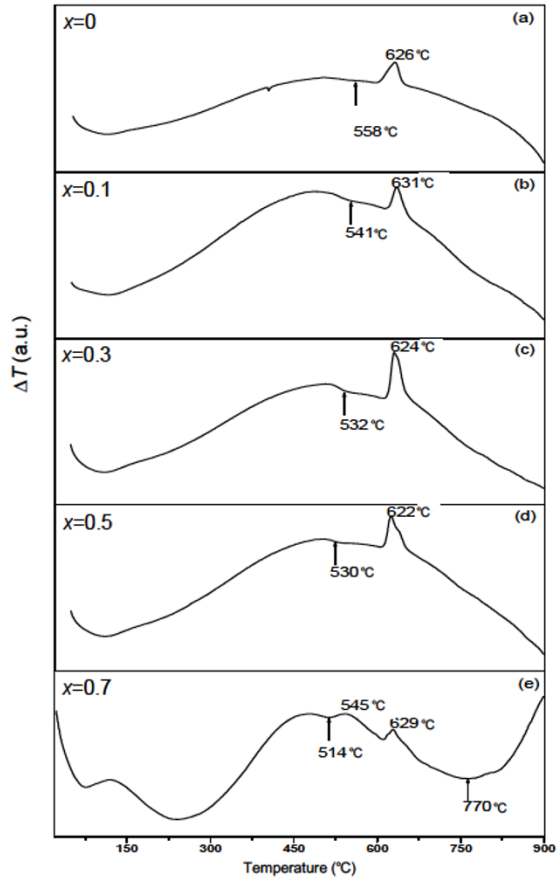

Fig. 2 DTA patterns of glass samples with (a) $x=0$, (b) $x=0.1$, (c) $x=0.3$, (d) $x=0.5$ and (e) $x=0.7$ in the glass system $55[(Pb_xBi_{1-x})TiO_3]$–$44[2SiO_2B_2O_3]$–La_2O_3.

T_{c1}, T_{c2} and T_{c3} at temperatures 545 ℃, 629 ℃ and 770 ℃, respectively. The peaks at T_{c1} and T_{c2} are observed exothermic in nature while the peak at T_{c3} is endothermic (Fig. 2(e)). The peak at T_{c1} for glass compositions $x=0$–0.5 represents the crystallization of the major bismuth titanium oxide ($Bi_2Ti_2O_7$) phase in all the glass ceramic samples. The DTA pattern of glass sample for $x=0.7$ (Fig. 2(e)) shows the peak at 545 ℃ due to some volatile impurity in the glass sample, not due to the crystallization of the major/minor phases, while the peaks at 629 ℃ and 770 ℃ are due to the crystallization of the $Bi_2Ti_2O_7$ (bismuth titanum oxide)/$Pb_3Bi_4Ti_6O_{21}$ (lead bismuth titanium oxide) phases. This is also confirmed by powder XRD studies that the peaks correspond to the crystallization of major phases of all the glasses.

3.4 X-ray diffraction analysis and crystallization behavior

XRD patterns for various glass ceramic samples crystallized at different temperatures with a heating rate of 5 ℃/min for 4 h are shown in Fig. 3. All the peaks in respective XRD patterns are matched with

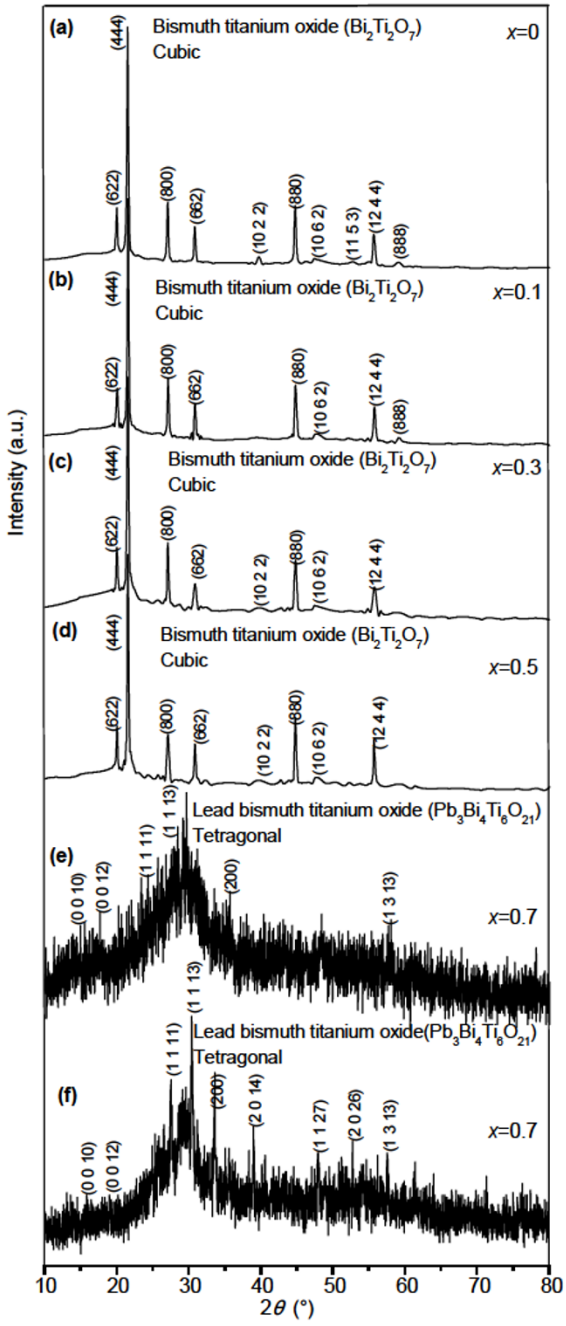

Fig. 3 XRD patterns of different glass ceramic samples: (a) BTL0.0626F, (b) PBTL0.1631F, (c) PBTL0.3624F, (d) PBTL0.5622F, (e) PBTL0.7629F and (f) PBTL0.7770F.

JCPDS Cards Nos. 32-0118 and 35-0007 of various compounds of constituent oxides. XRD pattern for the glass ceramic sample BTL0.0626F ($x=0$) is shown in Fig. 3(a). It is observed from the XRD pattern that bismuth titanium oxide ($Bi_2Ti_2O_7$, BTO) is the major crystalline phase for this glass ceramic sample. Figures 3(b) and 3(c) show the XRD patterns of glass ceramic samples PBTL0.1631F and PBTL0.3624F heat treated at different temperatures. The XRD pattern of glass ceramic sample PBTL0.1631F shows the presence of cubic phase of $Bi_2Ti_2O_7$ as a major phase. The XRD data of the major phase of glass ceramic samples rich in bismuth content ($x=0$–0.5) and glass ceramic samples rich in lead content ($x=0.7$) are indexed on the basis of cubic as well as tetragonal unit cells. Glass ceramic code, density, heating rate, holding time, holding temperature, crystal structure and crystalline phase are given in Table 2. The glass ceramic sample with $x=0.5$ obtained by the heat treatment at 622 ℃ is found to show the similar crystallization behavior of glass ceramic sample PBTL0.3624F (Fig. 3(c)), differing slightly only in terms of peak intensity and values of 2θ. The XRD patterns of glass ceramic samples PBTL0.7629F and PBTL0.7770F are shown in Figs. 3(e) and 3(f), respectively. The XRD patterns of these glass ceramic samples show the presence of tetragonal major phase of lead bismuth titanium oxide ($Pb_3Bi_4Ti_6O_{21}$, PBTO). Improved crystanality has been observed in the glass ceramic sample which is obtained by heat treating at 770 ℃ (PBTL0.7770F) in comparison to the glass ceramic sample obtained by heat treating at 629 ℃ (PBTL0.7629F). The crystallite size was calculated using Scherer formula [41]:

$$D_{\mathrm{p}}=\frac{K\lambda}{\beta\cos\theta} \tag{2}$$

where K is the shape factor (0.94); λ is the wavelength of Cu Kα line (1.54 Å); and β is the full width at half maximum. Glass ceramic sample code, average crystallite and grain size have been listed in Table 3. The minimum and maximum values of crystallite size corresponding to maximum intensity peaks of glass ceramic samples PBTL0.7629F and PBTL0.5622E have been found 1.10 nm and 66.09 nm, and their average crystallite size are 833 nm and 500 nm, respectively.

The XRD patterns for glass ceramic samples BTL0.0626E, PBTL0.1631E, PBTL0.3624E, PBTL0.5622E, PBTL0.7629E and PBTL0.7770E are shown in Fig. 4. Glass ceramic samples BTL0.0626E and PBTL0.1631E have the phase constitution similar to BTL0.0626F and PBTL0.1631F that obtained by heat treating for 4 h. For the glass ceramic sample PBTL0.3624E, a change is observed in the crystalline nature in the XRD pattern of this glass ceramic sample in comparison to the glass ceramic sample PBTL0.3624F. This change may be due to back ground noise and a new peak observed at 2θ value 14.8° corresponding to the plane (222). Similar crystallization behavior has been observed for glass ceramic sample PBTL0.5622E (Fig. 4(d)). The major phase of lead bismuth titanium oxide ($Pb_3Bi_4Ti_6O_{21}$, PBTO) is crystallized for the glass sample heat treated at 629 ℃ for 8 h. Further, for the same glass sample crystallized at 770 ℃ for 8 h heat treatment schedule, the major phase of PBTO crystallizes successfully; only a slight change has been observed in the XRD pattern of this glass ceramic sample in which broadness of the peak decreases showing the decrement in the amorphous nature of the glass ceramic sample. The XRD patterns of these glass ceramic samples crystallized for 4 h as well as 8 h heat treatment schedules along with SEM micrographs give adequate information about the morphology and crystallites size.

Table 3 Glass ceramic sample code, average crystallite and grain size

Glass ceramic sample code	Crystallite size (nm)	Grain size (nm)
BTL0.0626F	43.48	1250
BTL0.0626E	38.01	600
PBTL0.1631F	50.75	1250
PBTL0.1631E	60.93	500
PBTL0.3624F	30.43	500
PBTL0.3624E	27.67	750
PBTL0.5622F	50.75	1000
PBTL0.5622E	66.09	500
PBTL0.7629F	1.10	833
PBTL0.7629E	1.25	1250
PBTL0.7770F	2.51	1250
PBTL0.7770E	2.87	1250

3.5 Surface morphological analysis

The surface morphology of all glass ceramic samples shows fine crystallites of major phases of bismuth titanum oxide ($Bi_2Ti_2O_7$, BTO) and lead bismuth titanium oxide ($Pb_3Bi_4Ti_6O_{21}$, PBTO). Qualitative inspection of all these SEM micrographs reveals that the relative content of residual glass phase is present in

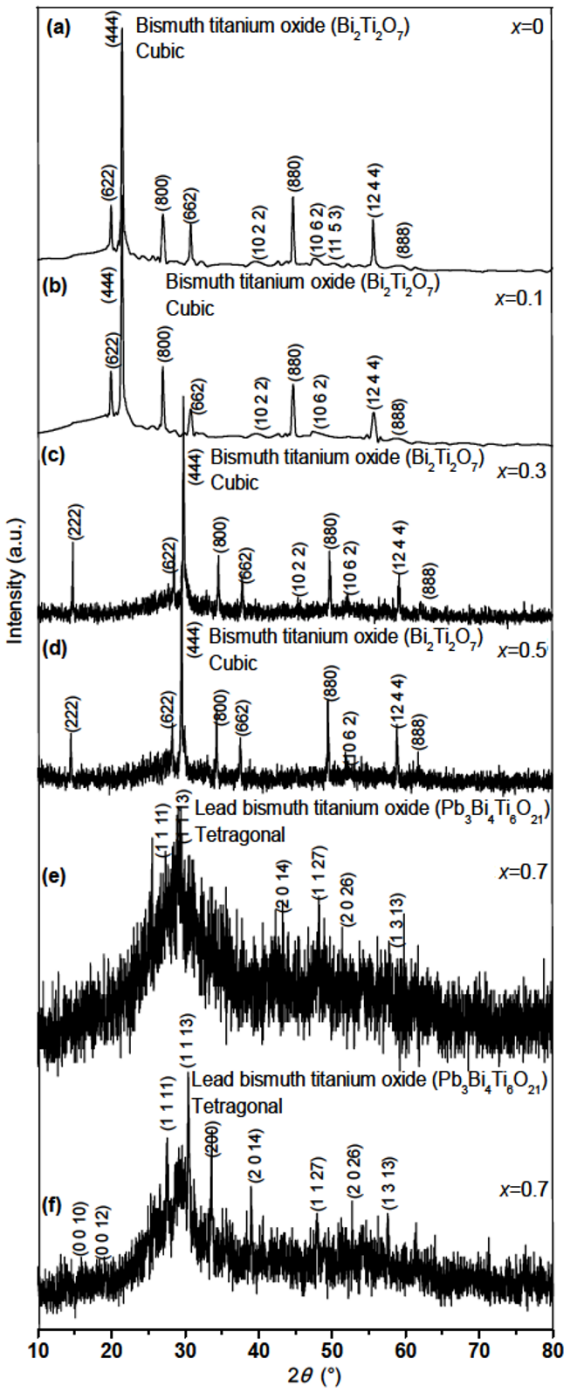

Fig. 4 XRD patterns of different glass ceramic samples: (a) BTL0.0626E, (b) PBTL0.1631E, (c) PBTL0.3624E, (d) PBTL0.5622E, (e) PBTL0.7629E and (f) PBTL0.7770E.

little amount or absent significantly in bismuth rich glass ceramic samples. The coexistence of coarse and fine particles has been also observed in all the glass ceramic sample micrographs similar to the lead titanate based glass–ceramics [42,43]. The SEM micrographs of various glass ceramic samples heat treated for 4 h and 8 h are shown in Figs. 5–7. Figure 5 shows SEM micrographs of glass ceramic samples BTL0.0626F, PBTL0.1631F, PBTL0.3624F, PBTL0.5622F, PBTL0.7629F and PBTL0.7770F. The glass ceramic sample BTL0.0626F is found to be composed of interconnected fine and uniform crystallites of bismuth titanum oxide ($Bi_2Ti_2O_7$, BTO), which are dispersed in the glassy matrix and separated by well developed grain boundaries throughout the micrograph (Fig. 5(a)). XRD studies confirm that the fine crystallites are BTO which is the major crystalline phase. In general, the white region in the microstructure represents the agglomerated major crystalline phase of BTO, while the black region depicts the residual glass in all SEM micrographs. For the glass ceramic sample PBTL0.1631F, there is a change in the morphology of the crystallites of the major phase BTO (Fig. 5(b)). These crystallites are found to have irregular shape and not uniformly distributed in the glassy matrix. Figure 5(c) shows the SEM micrograph of the glass ceramic sample PBTL0.3624F. The crystallite size has been found in the order of sub-micron range, while the volume fraction of the residual glass has been found large. The crystal growth and their distribution are not appearing properly in this micrograph. Figure 5(d) represents the SEM micrograph for the glass ceramic sample PBTL0.5622F. The glass ceramic sample PBTL0.5622F shows the cabbage-like crystallites are uniformly dispersed as a major phase of BTO along with trace amount of secondary phase in the glassy matrix.

Figures 5(e) and 5(f) depict the SEM micrographs for the glass ceramic samples PBTL0.7629F and PBTL0.7770F, respectively. Tetragonal lead bismuth titanium oxide ($Pb_3Bi_4Ti_6O_{21}$) is crystallized as the major phase for these glass ceramic samples. There are two types of phase formation seen in these micrographs: (i) tetragonal crystallites which are big in shape and size due to the large content of PbO ($x = 0.7$) and (ii) needle-like secondary phase due to the crystal growth of the bismuth oxide. When the same glass sample is crystallized at higher temperature 770 ℃, a slight change in the morphology has been found that the needle-like secondary phase is observed very less.

Figure 6 shows the SEM micrographs of different glass ceramic samples BTL0.0626E, PBTL0.1631E, PBTL0.3624E and PBTL0.3624E (at lower magnification). These glass ceramic samples are obtained through crystallization of their parent glasses for 8 h heat treatment schedule. The entire morphology

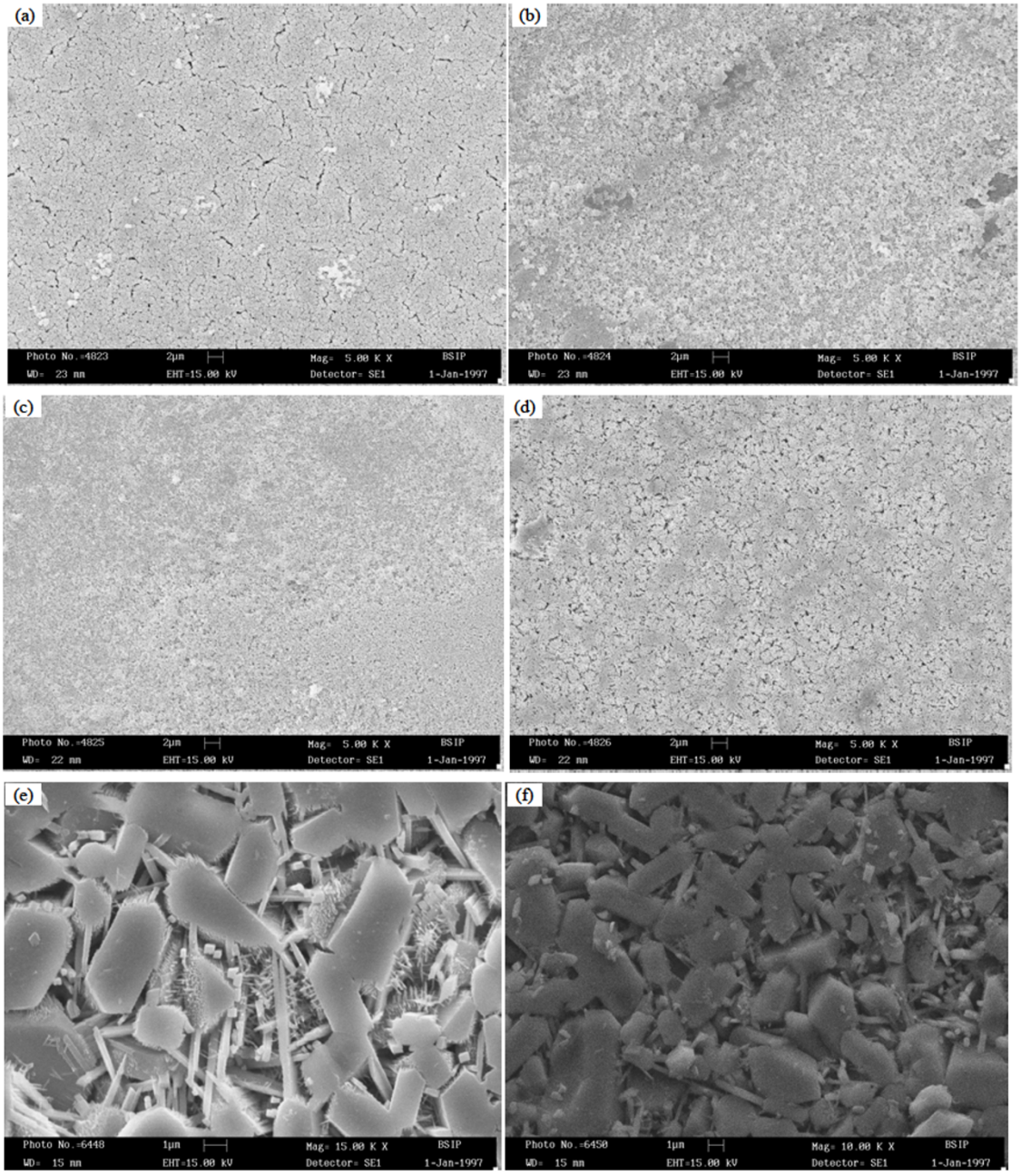

Fig. 5 SEM micrographs of glass ceramic samples: (a) BTL0.0626F, (b) PBTL0.1631F, (c) PBTL0.3624F, (d) PBTL0.5622F, (e) PBTL0.7629F and (f) PBTL0.7770F.

has been found to be changed in comparison to the 4 h heat treated glass ceramic samples with the same compositions, which are not clear from XRD studies. Figures 6(a) and 6(b) depict the SEM micrographs of the glass ceramic samples BTL0.0626E and PBTL0.1631E. The morphology of the crystallites is found similar, but they are differing in terms of the crystal growth and their distribution. The well developed, interconnected and dense crystallites of the major phase of BTO are dispersed uniformly in the glassy matrix, while the crystal growth for the glass ceramic sample PBTL0.1631E ($x=0.1$) are not well developed and the agglomeration of the crystallites are also observed. Figures 6(c) and 6(d) show the micrographs of the glass ceramic sample PBTL0.3624E at different magnifications. Very sharp and fine needle-like crystal growth of major phase of BTO has been observed along with secondary phase. When we take the micrograph of the same glass ceramic sample PBTL0.3624E at lower magnification, the secondary phase is clearly seen in different shape and size.

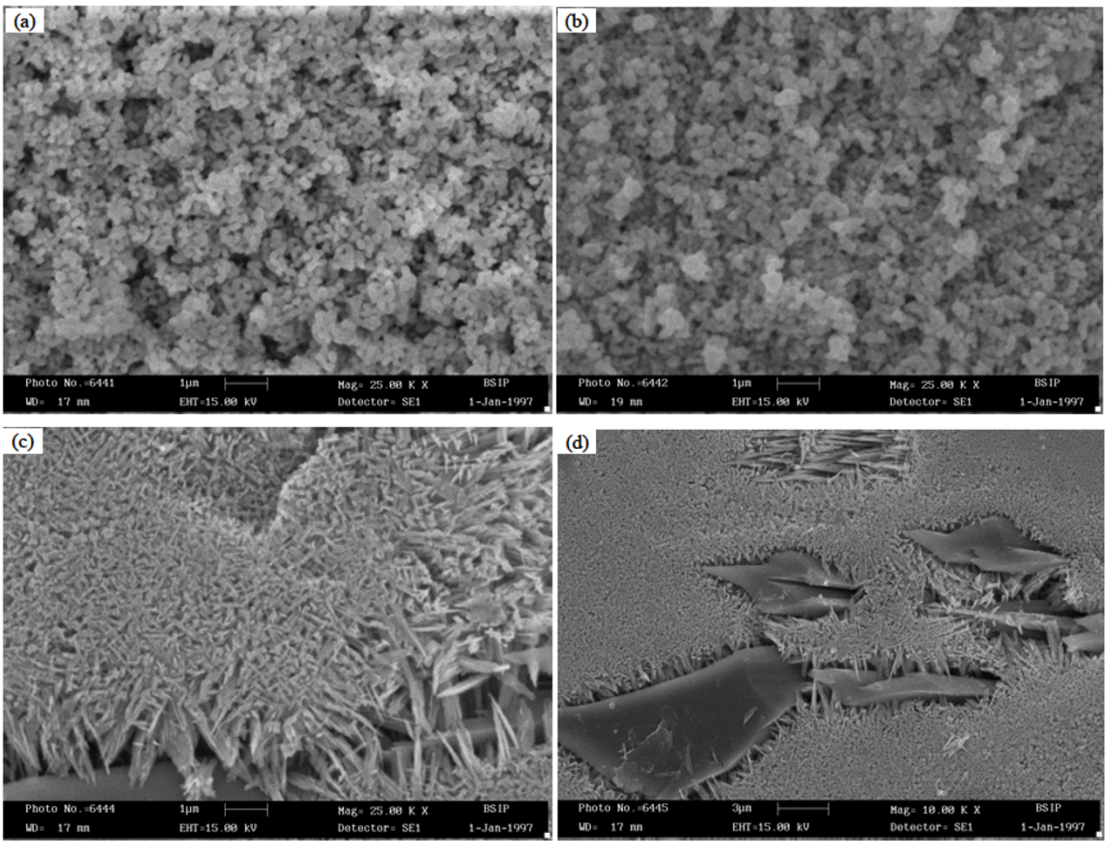

Fig. 6 SEM micrographs of glass ceramic samples: (a) BTL0.0626E, (b) PBTL0.1631E, (c) PBTL0.3624E and (d) PBTL0.3624E (at lower magnification).

Figure 7 shows the SEM of glass ceramic samples PBTL0.5622E, PBTL0.7629E, and PBTL0.770E respectively. Figure 7(a) represents the micrograph of the glass ceramic sample PBTL0.5622E which is obtained by 8 h heat treatment schedule of the same parent glass sample. Very fine crystal growth has been observed along with needle-like secondary phase. If we compare this micrograph with 4 h heat treated glass ceramic sample (Fig. 5(d)), the grain boundary seems to be disappearing and interconnected to each other for 8 h heat treated glass ceramic sample. Figures 7(c) and 7(d) show the similar morphology of the glass ceramic samples heat treated for 4 h.

3.6 Dielectric behavior

Dielectric constant ε_r and dissipation factor D were measured as a function of temperature within the temperature range of 50–320 ℃ at various selected frequencies such as 20 Hz to 1.0 MHz for tentative glass ceramic samples PBTL0.3624F and PBTL0.5622F. Figure 8 shows the variations of ε_r and D with temperature for glass ceramic sample PBTL0.3624F. Initially, the value of ε_r has been found constant up to a certain value of temperature 200 ℃, and thereafter, it increases with increasing temperature at low frequency range from 20 Hz to 1 kHz, while the value of ε_r is found constant meaning temperature independent at the high frequency range. The value of dielectric constant ε_r and dissipation factor D at temperature 60 ℃ at 1 kHz have been found to be 32 and 0.0013, respectively. Almost similar behavior has been observed for the plot of dissipation factor D vs. temperature. The maximum value of dielectric constant is found to be the order of 500 along with dissipation factor value 1.2.

Figure 9 shows the plots of dielectric constant ε_r and dissipation factor D vs. temperature for the glass ceramic sample PBTL0.5622F. Both the plots has similar trends and increase in ε_r and D, which may be due to increase in the electrical conduction with increasing temperature [44]. The dielectric behavior of this glass ceramic sample can be explained in terms of the addition of La_2O_3 which promotes the crystallization of the glass during the heat treatment. A small concentration of donor dopant La^{3+} in perovskite ceramics is known to induce an n-type

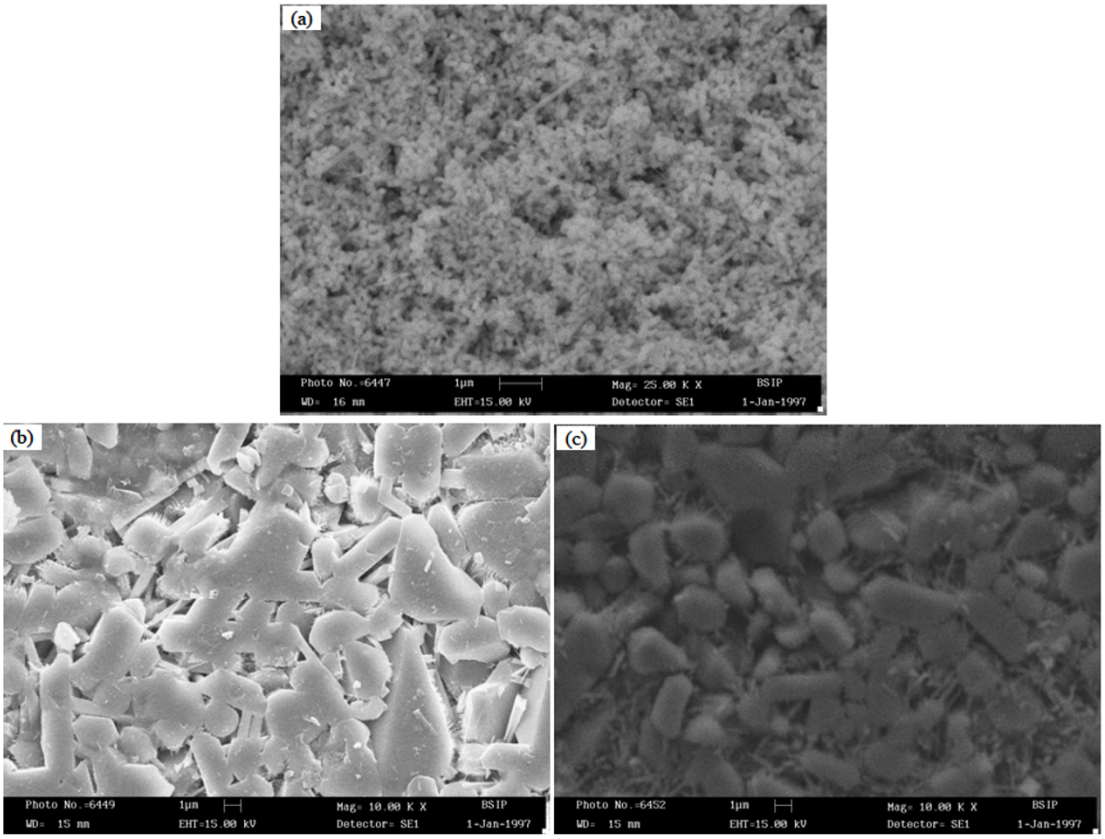

Fig. 7 SEM micrographs of glass ceramic samples: (a) PBTL0.5622E, (b) PBTL0.7629E and (c) PBTL0.770E.

semiconductivity by electronic compensation.

$$La^{3+} \xrightarrow{BiTiO_3} La^{\bullet}_{Sr} + e' \quad (3)$$

Due to the difference in conductivity, interfacial polarization arises at crystal–glass interface and attributes to high value of dielectric constant ε_r. This causes the effective value of ε_r with the order of 1100 [45]. The increase in the value of dielectric constant with increasing temperature at 0.1 kHz to 1 kHz for these glass ceramic samples might be due to the increasing concentration of Bi^{2+} in the parent glass compositions. The dielectric constant as well as loss data shows that with increasing value of x (content of PbO) in the glasses, ε_r and loss values are increased gradually. This increase in ε_r and D values is attributed to the expending concentration of alkali ion charge carriers with increase of PbO content in the glass in expense of SiO_2. Electrical property of a glass is primarily controlled by the connectivity of the continuous glassy phase, and this glass phase is reduced and crystalline phases are increased after heat treatment. It is observed that glass ceramic sample PBTL0.5622F contains less crystal compared to the glass ceramic sample PBTL0.3624F, and its dielectric loss is more compared to PBTL0.5622F. Murugan *et al*. [2] have also observed that the dielectric loss D decreases with increasing ferroelectric phases in the glass–ceramics, and they also reported that D value is less for glasses compared to the polycrystalline ceramics in the same system.

4 Conclusions

DTA patterns of the Bi rich glass samples show only single exothermic peak, while DTA patterns of the Pb rich glass samples show more than one exothermic peak as well as one endothermic peak. DTA peak at T_c for all glass samples shifts towards lower temperature side due to the different melting temperature and viscosity of the melts. The XRD patterns of Bi rich glass ceramic samples show the major phase of bismuth titanum oxide ($Bi_2Ti_2O_7$), while it is observed for Pb rich glass ceramic samples as lead bismuth titanium oxide ($Pb_3Bi_4Ti_6O_{21}$). Crystalline phase of all the glass ceramic samples with $0 \leqslant x \leqslant 0.5$ is found to have cubic crystal structure, and for $x = 0.7$ it is observed tetragonal crystal structure. The effect of heat

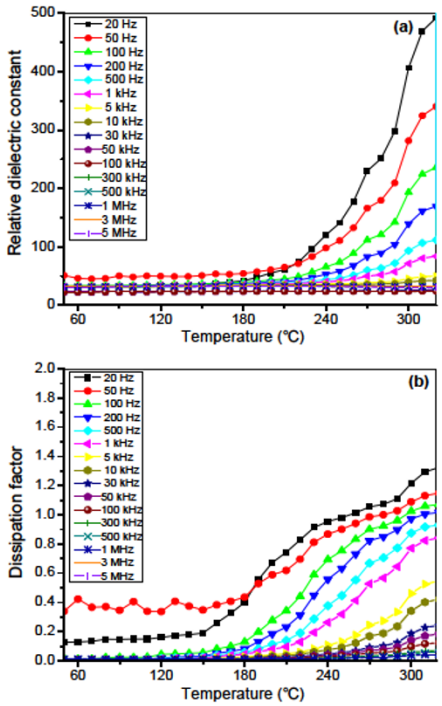

Fig. 8 Variations of (a) dielectric constant ε_r and (b) dissipation factor D with temperature at different frequencies for the glass ceramic sample PBTL0.3624F.

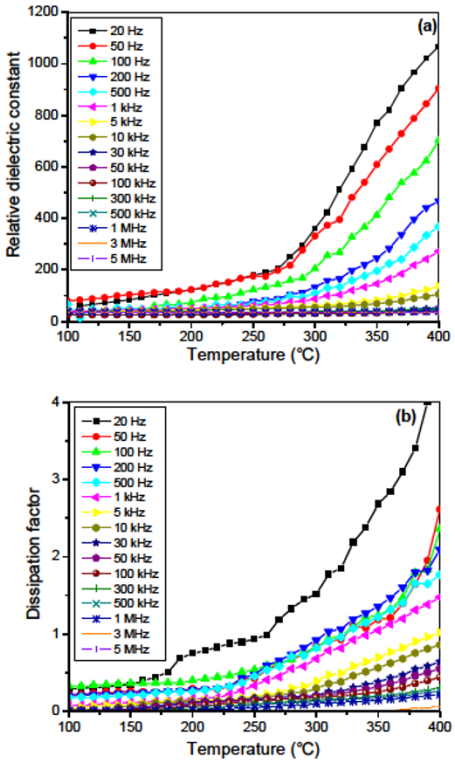

Fig. 9 Variations of (a) dielectric constant ε_r and (b) dissipation factor D with temperature at different frequencies for the glass ceramic sample PBTL0.5622F.

treatment schedule for 4 h and 8 h changes the surface morphology of the crystallites. XRD results reveal that the heat treatment schedules are found to be the same for 4 h and 8 h. It is also concluded that the value of dielectric constant is found larger for glass ceramic sample PBTL0.5622F in comparison to the glass ceramic sample PBTL0.3624F.

Acknowledgements

The authors are gratefully acknowledged to the Uttar Pradesh Council of Science and Technology, Lucknow (India) for financial support under the "Young Scientist Scheme" as major research project No. CSTT/YSS/D-3913. Authors are also thankful to Dr. Atul Khanna, associate professor, for his constant support and to extending the XRD measurement facility at Department of Physics, Guru Nanak Dev University, Amritsar 143005, India.

References

[1] Aurivillius B. Mixed bismuth oxides with layer lattices. II. Structure of $Bi_4Ti_3O_{12}$. *Arkiv for Kemi* 1949, **1**: 499–512.

[2] Murugan GS, Subbanna GN, Varma KBR. Nanocrystallization of ferroelectrics bismuth tungstate in lithium borate glass matrix. *J Mater Sci Lett* 1999, **18**: 1687–1690.

[3] Borrelli NF, Layton MM. Electrooptic properties of transparent ferroelectric glass–ceramic systems. *IEEE T Electron Dev* 1969, **16**: 511–514.

[4] Bell AJ. Ferroelectrics: The role of ceramic science and engineering. *J Eur Ceram Soc* 2008, **28**: 1307–1317.

[5] Pengpat K, Holland D. Ferroelectric glass–ceramics from the $PbO–GeO_2–Nb_2O_5$ system. *J Eur Ceram Soc* 2004, **24**: 2951–2958.

[6] Graça MPF, da Silva MGF, Valente MA. Structural and electrical properties of $SiO_2–Li_2O–Nb_2O_5$ glass and glass–ceramics obtained by thermoelectric treatments. *J Mater Sci* 2007, **42**: 2543–2550.

[7] Graça MPF, Valente MA, da Silva MGF. The electric behavior of a lithium–niobate–phosphate glass and glass-ceramics. *J Mater Sci* 2006, **41**: 1137–1141.

[8] Shankar MV, Varma KBR. Crystallization of ferroelectric bismuth vanadate in Bi_2O_3–V_2O_5–SrB_4O_7 glasses. *J Non-Cryst Solids* 1998, **226**: 145–154.

[9] Pengpat K, Holland D. Glass-ceramics containing ferroelectric bismuth germanate (Bi_2GeO_5). *J Eur Ceram Soc* 2003, **23**: 1599–1607.

[10] Ruiz-Valdés JJ, Gorokhovsky AV, Escalante-García JI, *et al*. Glass-ceramic materials with regulated dielectric properties based on the system BaO–PbO–TiO_2–B_2O_3–Al_2O_3. *J Eur Ceram Soc* 2004, **24**: 1505–1508.

[11] Bengisu M, Brow RK, Wittenauer A. Glasses and glass–ceramics in the SrO–TiO_2–Al_2O_3–SiO_2–B_2O_3 system and the effect of P_2O_5 additions. *J Mater Sci* 2008, **43**: 3531–3538.

[12] Subbarao EC. A family of ferroelectric bismuth compounds. *J Phys Chem Solids* 1962, **23**: 665–676.

[13] De Araujo CA, Cuchiaro J, Mcmillan LD, *et al*. Fatigue-free ferroelectric capacitors with platinum electrodes. *Nature* 1994, **374**: 627–629.

[14] Park BH, Kang BS, Bu SD, *et al*. Lanthanum-substituted bismuth titanate for use in non-volatile memories. *Nature* 1999, **401**: 682–684.

[15] Takenaka T, Nagata H. Current status and prospects of lead-free piezoelectric ceramics. *J Eur Ceram Soc* 2005, **25**: 2693–2700.

[16] Kojima S, Hushur A, Jiang F, *et al*. Crystallization of amorphous bismuth titanate. *J Non-Cryst Solids* 2001, **293–295**: 250–254.

[17] Sunahara K, Yano J, Kakegawa K. Preparation of $Bi_4Ti_3O_{12}$ particles by crystallization from glass. *J Eur Ceram Soc* 2006, **26**: 623–626.

[18] Gerth K, Rüssel C. Crystallization of $Bi_4Ti_3O_{12}$ from glasses in the system Bi_2O_3/TiO_2/B_2O_3. *J Non-Cryst Solids* 1997, **221**: 10–17.

[19] Bruton TM. Study of the liquidus in the system Bi_2O_3–TiO_2. *J Solid State Chem* 1974, **9**: 173–175.

[20] Gerth K, Rüssel C. Crystallization of Bi_3TiNbO_9 from glasses in the system Bi_2O_3/TiO_2/Nb_2O_5/B_2O_3/SiO_2. *J Non-Cryst Solids* 1999, **243**: 52–60.

[21] Krapchanska M, Dimitriev Y, Iordanova R. Phase formation in the system Bi_2O_3–TiO_2–SiO_2. *Journal of the University of Chemical Technology and Metallurgy* 2006, **41**: 307–310.

[22] Tang Q-Y, Kan Y-M, Wang P-L, *et al*. Nd/V co-doped $Bi_4Ti_3O_{12}$ power prepared by molten salt synthesis. *J Am Ceram Soc* 2007, **90**: 3353–3356.

[23] Kojima T, Sakai T, Watanabe T, *et al*. Large remanent polarization of $(Bi,Nd)_4Ti_3O_{12}$ epitaxial thin films grown by metalorganic chemical vapor deposition. *Appl Phys Lett* 2002, **80**: 2746.

[24] Kim JK, Kim SS, Kim W-J. Effects of annealing conditions on the electrical properties of $Bi_{4-x}Nd_xTi_3O_{12}$ (x = 0.46) thin films processed at low temperature. *Appl Phys A* 2006, **82**: 737–740.

[25] Sakamoto W, Yamada M, Iizawa N, *et al*. Preparation and properties of $Bi_{4-x}Nd_xTi_3O_{12}$ thin films by chemical solution deposition. *J Electroceram* 2004, **13**: 339–343.

[26] Wu D, Li A, Ming N. Structure and electrical properties of of $Bi_{3.15}Nd_{0.85}Ti_3O_{12}$ ferroelectric thin films. *J Appl Phys* 2004, **95**: 4275.

[27] Maiwa H, Iizawa N, Togawa D, *et al*. Electromechanical properties of Nd-doped $Bi_4Ti_3O_{12}$ films: A candidate for lead-free thin-film piezoelectics. *Appl Phys Lett* 2003, **82**: 1760–1762.

[28] Suyal G, Bharadwaja SSN, Cantoni M, *et al*. Properties of chemical solution deposited polycrystalline neobidium-modified $Bi_4Ti_3O_{12}$. *J Electroceram* 2002, **9**: 187–192.

[29] Gao XS, Xue JM, Wang J. Ferroelectric behavior and charge carriers in Nd-doped $Bi_4Ti_3O_{12}$ thin films. *J Appl Phys* 2005, **97**: 034101.

[30] Chen M, Liu ZL, Wang Y, *et al*. Ferroelectric properties and microstructures of Nd_2O_3-doped $Bi_4Ti_3O_{12}$ ceramics. *Phys Status Solidi a* 2003, **200**: 446–450.

[31] Vernacotala DE, Chatlani S, Shelby JE. Applications of ferroelectrics. *Proceedings of the 12th IEEE International Symposium on Applications of Ferroelectric*. Honolulu, Hawaii, USA, 2000.

[32] Shankar MV, Varma KBR. Crystallization, dielectric and optical studies on strontium tetraborate glasses containing bismuth titanate. *Mater Res Bull* 1998, **33**: 1769–1782.

[33] Molla AR, Tarafder A, Karmakar B. Synthesis and properties of glasses in the K_2O–SiO_2–Bi_2O_3–TiO_2 system and bismuth titanate ($Bi_4Ti_3O_{12}$) nano glass–ceramics thereof. *J Mater Sci* 2011, **46**: 2967–2976.

[34] Golezardi S, Marghussian VK, Beitollahi A, *et al*. Crystallization behavior, microstructure and dielectric properties of lead titanate glass ceramics in the presence of Bi_2O_3 as a nucleating agent. *J Eur Ceram Soc* 2010, **30**: 1453–1460.

[35] Reddy AA, Tulyaganov DU, Kapoor S, *et al*. Study of melilite based glasses and glass–ceramics nucleated by Bi_2O_3 for functional applications. *RSC Adv* 2012, **2**: 10955–10967.

[36] El-Meliegy E, van Noort R. *Glasses and Glass Ceramics for Medical Applications*. New York: Springer, 2012.

[37] Gautam CR, Kumar D, Parkash O. Controlled

crystallization of (Pb,Sr)TiO_3 borosilicate glass ceramics doped with Nb_2O_5. *Glass Phys Chem+* 2013, **39**: 162–173.

[38] Gautam CR, Kumar D, Parkash O. Crystallization behavior and microstructural analysis of lead-rich $(Pb_xSr_{1-x})TiO_3$ glass ceramics containing 1 mole% La_2O_3. *Advances in Materials Science and Engineering* 2011, **2011**: 402376.

[39] Gautam CR, Kumar D, Parkash O. Crystallization behavior and microstructural analysis of strontium-rich $(Pb_xSr_{1-x})TiO_3$ glass ceramics in presence of La_2O_3. *Advances in Materials Science and Engineering* 2011, **2011**: 747346.

[40] Gautam CR, Yadav AK, Singh P. Synthesis, crystallization and microstructural study of perovskite (Ba,Sr)TiO_3 borosilicate glass ceramic doped with La_2O_3. *Mater Res Innov* 2013, **17**: 148–153.

[41] Patterson AL. The Scherrer formula for X-ray particle size determination. *Phys Rev* 1939, **56**: 978–982.

[42] Sahu AK, Kumar D, Parkash O. Crystallization of lead strontium titanate perovskite phase in $[(Pb_{1-x}Sr_x)O{\cdot}TiO_2]$–$[2SiO_2{\cdot}B_2O_3]$–$[K_2O]$ glass ceramics. *Adv Appl Ceram* 2003, **102**: 139–147.

[43] Bahramia A, Nemati ZA, Alizadeh P, *et al*. Crystallization and electrical properties of $[(Pb_{1-x}Sr_x){\cdot}TiO_3][(2SiO_2{\cdot}B_2O_3)][K_2O]$ glass–ceramics. *J Mater Process Tech* 2008, **206**: 126–131.

[44] Kumar D, Gautam CR, Parkash O. Preparation and dielectric characterization of ferroelectric $(Pb_xSr_{1-x})TiO_3$ glass ceramics doped with La_2O_3. *Appl Phys Lett* 2006, **89**: 112908.

[45] Gautam CR, Singh P, Thakur OP, *et al*. Synthesis, structure and impedance spectroscopic analysis of $[(Pb_xSr_{1-x}){\cdot}OTiO_2]$–$[(2SiO_2{\cdot}B_2O_3)]$–7[BaO]–3$[K_2O]$ glass ceramic system doped with La_2O_3. *J Mater Sci* 2012, **47**: 6652–6664.